A Room-Temperature Molten Hydrate Electrolyte for Rechargeable Zinc–Air Batteries

Chih-Yao Chen, Kazuhiko Matsumoto, Keigo Kubota, Rika Hagiwara, and Qiang Xu**

Dr. C. Y. Chen, Prof. K. Matsumoto, Dr. K. Kubota, Prof. R. Hagiwara, Prof. Q. Xu
AIST-Kyoto University Chemical Energy Materials Open Innovation Laboratory (ChEM-OIL)
National Institute of Advanced Industrial Science and Technology (AIST)
Yoshida, Sakyo-ku, Kyoto 606-8501, Japan
E-mail: keigo-kubota@aist.go.jp
E-mail: q.xu@aist.go.jp

Prof. K. Matsumoto, Prof. R. Hagiwara
Graduate School of Energy Science
Kyoto University
Yoshida, Sakyo-ku, Kyoto 606-8501, Japan

Dr. K. Kubota, Prof. Q. Xu
Research Institute of Electrochemical Energy
National Institute of Advanced Industrial Science and Technology (AIST)
Ikeda, Osaka 563-8577, Japan

Keywords: molten hydrates, ionic liquids, zinc anodes, aqueous batteries, zinc–air batteries

Aqueous Zn-based batteries are attracting extensive interest because of their economic feasibility and potentially high energy density. However, poor rechargeability of Zn anode in conventional electrolytes resulting from dendrite formation and self-corrosion hinders the practical implementation. Herein, a Zn molten hydrate composed of inorganic Zn salt and water is demonstrated as an advantageous electrolyte for solving these issues. In this electrolyte, dendrite-free Zn deposition/dissolution reaction with a high coulombic efficiency (~99%) as well as long-term stability free from CO_2 poisoning are realized. The resultant Zn–air cell exhibits a reversible capacity of 1000 mAh $g_{(catalyst)}^{-1}$ over 100 cycles at 30 °C. Combined with the intrinsic safety associated with aqueous chemistry and cost benefit of the raw material, the present Zn–air battery makes a strong candidate for large-scale energy storage.

Since their commercialization, lithium-ion batteries (LIBs) have dominated the field of portable electronic devices for decades. Scaling up of LIBs to fully electrify automotives as well as to store and regulate intermittent renewable energy sources, however, encounters great challenges owing to the projected cost,[1] and safety concerns caused by the use of flammable organic electrolytes.[2] Against this background, rechargeable batteries employing metallic Zn as the anode warrant special attention owing to the following reasons;[3,4] the abundance and large production of Zn make it economically viable, the applicability of aqueous electrolytes grants an intrinsic safety, and its low reactivity and ease of handling are also advantageous for battery manufacturing process. In order to compensate the moderate redox potential of Zn/Zn^{2+} (–0.76 V vs standard hydrogen electrode (SHE)) compared to Li/Li^{+} (–3.04 V vs SHE), research efforts in this realm have spanned from intercalation chemistry[3–7] to conversion reaction, namely, Zn–air batteries.[8–12] The most notable characteristic of the latter configuration is the utilization of an ideally inexhaustible cathode reactant, oxygen, from the ambient atmosphere, which renders it prominent theoretical capacities in both gravimetric and volumetric criteria.[12] Efforts toward rechargeable Zn–air batteries so far mainly focused on the developments of bifunctional catalyst cathode materials for facilitating oxygen reduction reaction (ORR) and oxygen evolution reaction (OER), with alkaline electrolytes (i.e., 6–7 M KOH) widely used to achieve fast electrode kinetics.[8–11] However, Zn anodes are prone to form dendrite and suffer from passivation and corrosion in a basic environment.[12–14] This situation is further complicated by the solid-solute-solid mechanism ($Zn–Zn(OH)_4^{2-}–ZnO$) and the degradation of alkaline electrolyte upon operation owing to carbon dioxide poisoning and water consumption.[12–14]

Although Zn deposition/dissolution reaction is as important as ORR/OER performance in determining the overall properties of a battery, only few attempts to ameliorate the anode reversibility were demonstrated. The strategy includes i) the use of neutral/acidic aqueous electrolytes to avoid the carbonization of electrolytes and reduce dendrite,[4,15,16] ii) surface

modification of Zn electrode with the aims to prevent passivation or homogenize current distribution,[17] and iii) a combination of them.[18,19] Recently, a pioneering work by Xu and Wang groups reported a nearly 100% coulombic efficiency of Zn deposition/dissolution employing a superconcentrated, so-called "water-in-salt" electrolytes, in which the unique solvation structure of Zn^{2+} contributed to the remarkable Zn reversibility.[20] However, typical Zn salts required for these studies are trifluoromethanesulfonate (TfO)[5–7,15,18,19] or bis(trifluoromethanesulfonyl)amide (TFSA).[20] These organic fluorinated salts are costly, which makes their practical application challenging and inevitably lessens the economic benefits anticipated for Zn-based batteries.[21] The existence of excess reaction-irrelevant ions in the electrolyte may also reduce the energy efficiency. Most importantly, the long-term reliability of Zn in most of these electrolytes is still far from satisfactory.[21]

Herein, we report a Zn–air battery with the utilization of an affordable Zn molten hydrate electrolyte to address the above issues (**Figure 1**a and b). Zinc chloride has been known for a century as one of the most water-soluble inorganic metal salts.[22] In the extremely concentrated state, the binary mixture is defined as zinc molten hydrate or hydrate melt (Figure S1, supporting information),[23] with all water molecules participating in Zn^{2+} hydration shells. As such, it is no longer an aqueous solution but rather close to an ionic liquid.[24,25] The wide liquidus composition range of $ZnCl_2$–H_2O system at ambient temperature serves as an ideal platform to elucidate the relationship between the solvation structure of Zn salts and its electrochemical behavior. It is worthwhile to emphasize that the water-in-salt electrolytes[26,27] are not molten hydrate, because they still contain non-negligible amount of free water molecules.[28,29] Using Zn molten hydrate as an electrolyte, dendrite-free stable cycling of Zn anodes over 4000 cycles was achieved. This electrolyte was shown to effectively suppress Zn corrosion and thus an improved battery shelf life is expectable. The resultant Zn–air batteries was demonstrated to give a reversible capacity of 1000 mAh g^{-1} (on the base of cathode active material mass) for 100 cycles. Lastly, as many low-melting inorganic molten hydrates are

known,[29] the present study may provide guidelines for the development of a new class of electrolytes for metal deposition and energy-related applications.

Cyclic voltammetry (CV) was performed to evaluate the Zn electrochemistry in a series of $ZnCl_2 \cdot nH_2O$ (n = 50, 10, 4, 3, 2.33), where a tungsten wire was used as the working electrode and Zn as the reference and counter electrode in a three-electrode setup. In all electrolytes, the cathodic peak below 0 V (vs Zn/Zn^{2+}) and the anodic peak around the open-circuit voltage (OCV) observed are associated with Zn deposition and dissolution, respectively (Figure S2).[30] These CV profiles superpose well during cycling, indicating the good reversibility of Zn redox reactions. X-ray diffraction (XRD) patterns of the deposits obtained at –0.2 V (vs Zn/Zn^{2+}) are presented in Figure S3. It reveals that the deposits are crystalline Zn without any impurity phase. It is interesting to notice an increased relative intensity of 002 to 101 indices when the stoichiometric water molar ratio is lower than 4. This implies that the preferential deposition of Zn is altered depending on the solution structure (vide infra). Scanning electron microscopy (SEM) images of Zn deposits are shown in Figure 1c. Conspicuously, the morphology transforms from fine-size dendrites to well-defined hexagonal crystals as water content decreases. The high Zn concentration in molten hydrate electrolytes is supposed to significantly alleviate the establishment of cocnentration gradient during the deposition process, and the stable ion supply to the Zn anode favors the uniform deposition. The bulk and dense nature of the Zn deposit obtained in molten hydrate electrolytes is beneficial for complete dissolution. Zn deposits of similar morphology and crystallographic feature were obtained with the aid of an ionic liquid electrolyte.[31] In addition, the anodic stability is improved as water content decreases, which is possibly owing to the smaller amount of uncoordinated water causing the side reaction (Figure S4). On the other hand, the Zn redox reaction within the alkaline electrolyte (6 M KOH-0.2 M $ZnCl_2$) exhibits low reversibility as known before (Figure S5).[4,15] The inferior coulombic efficiency could be ascribed to the proton reduction that simultaneously

occurred during Zn electrodeposition,[32] along with the highly porous and non-adherent microstructure of the Zn deposit (Figure S5).

Among the electrolytes investigated, the ionic conductivity of $ZnCl_2 \cdot nH_2O$ reaches a maximum at $n = 10$ and decreases with increasing $ZnCl_2$ content (**Figure 2**a). The drop in the bulk conductivity suggests that the addition of $ZnCl_2$ gives rise to increase in ionic interactions and interferes the liquid dynamics.[33] Nevertheless, a reasonably high value of 15 mS cm^{-1} is attained at the most concentrated $ZnCl_2 \cdot 2.33H_2O$ at 30 °C. This value is higher than that of most of ionic liquids[34] and is comparable to conventional Li-based nonaqueous electrolytes.[35] Figure 2b shows differential scanning calorimetry (DSC) thermograms for $ZnCl_2 \cdot nH_2O$. All electrolytes are proved to be liquid at room temperature (melting temperature ≤ 10 °C). Furthermore, their melting points observed are reproducible and well consistent with the previously reported phase diagram,[22,25] confirming that the stoichiometric ratios of our samples are reliable. Selected physicochemical properties of $ZnCl_2 \cdot nH_2O$ electrolytes studied are presented in Table S1. From the viewpoint of ambient temperature energy storage and/or electrodeposition, further concentrated system is not appropriate because the liquidus temperature increases with increasing $ZnCl_2$ content (e.g., 28.2 °C for $ZnCl_2 \cdot 1.8H_2O$, Table S1 and Figure S6).

To characterize the liquid structure at each $ZnCl_2/H_2O$ ratio, Raman spectra were obtained and the peaks were assigned according to previous reports (Figure 2c).[36–39] In the 3200-cm^{-1} region, Raman spectrum of the neat water shows a broad band originated from O–H stretching of water molecules.[39] The two bands at 280–320 cm^{-1} and 390–400 cm^{-1} are assigned to the symmetric stretching modes of the tetrahedral $[ZnCl_4]^{2-}$ and the octahedral aquo-complex $[Zn(OH_2)_6]^{2+}$, respectively.[36,37] With the increase of $ZnCl_2$ content, the $[ZnCl_4]^{2-}$ peak is gradually intensified at the expense of the O–H stretching band. Concomitantly, the H–O–H bending mode at 1650 cm^{-1} shows red shift and the peak becomes sharpened. This is the result of the structure breaking effect of Cl^- on the H bonding network between water molecules.[40]

Besides, a band assigned to the stretching mode of lower chloro-complexes of Zn^{2+} (e.g., $[ZnCl_3]^-$)[37,38] appears around 330 cm^{-1} as a shoulder overlapping the predominant $[ZnCl_4]^{2-}$ band. These observations are in qualitative agreement with previous measurements[37,38,41] and directly indicate that the bulk water nature is diminished in the $ZnCl_2$ concentrated states (n = 4, 3, 2.33). Consequently, the Zn surface chemistry and double-layer structure can be tailored by controlling the $ZnCl_2$ content, which leads to the favorable deposit morphology of Zn.[31] For the most concentrated $ZnCl_2 \cdot 2.33H_2O$, a new band at 230 cm^{-1} is discernible. This band is derived from the polynuclear aggregation of $[ZnCl_4]^{2-}$ via Cl^-, [36] which resembles molten $ZnCl_2$.[42] At this composition, the average number of coordinating water around Zn is less than 6 and thus incomplete hydration shells are formed. In addition, it is considered that competition between the Cl^- and water molecules for positions adjacent to Zn^{2+} occurs.[23] Compared to other compositions ($n \geq 3$), the peculiar solution structure and competing association between Cl^- and H_2O within $ZnCl_2 \cdot 2.33H_2O$ are supposed to affect the ion conduction behavior and the electrochemical characteristics. It was reported that the transference number of Zn ionic species decreased from +0.33 to –0.52 as the $ZnCl_2$ concentration increased from 0.5 to 12 M.[43] The negative transference number indicates that at higher $ZnCl_2$ concentrations most of the Zn ions are in the form of anionic complexes, and this can happen in molten hydrate electrolytes.[43,44]

Coulombic efficiency (C.E.) is an important parameter for any rechargeable batteries and is defined here as the ratio of the amount of Zn stripped from the working electrode versus the amount that is plated.[45] To evaluate it, coin cells were assembled with molybdenum working and Zn counter electrodes. The ten-cycle averaged coulombic efficiency in $ZnCl_2 \cdot 2.33H_2O$ is 98.7% after the initial two conditioning cycles (**Figure 3**a).[46] This value significantly outperformed that (C.E.< 50%) in the alkaline electrolyte under the same condition (Figure 3b). The inferior coulombic efficiency reflects that the majority of Zn deposit in the alkaline electrolyte is electrochemically inactive (dead Zn) and/or parasitic reactions occur. Symmetric Zn/Zn cells were further fabricated to study the long-term cycling performance. Figure 3c

shows the discharge-charge profiles using the $ZnCl_2 \cdot 2.33H_2O$ electrolyte at various current densities and a fixed areal capacity of 1 mAh cm^{-2}. At a current density of 1 mA cm^{-2}, the Zn/Zn cell could be durably cycled for 1000 h, with an overpotential less than 100 mV. At higher current density of 2 and 5 mA cm^{-2}, the cell could still give a stable capacity over 1000 h. Notably, the cell could even sustain cycling at a demanding condition of 10 mA cm^{-2} for 800 h, corresponding to 4000 cycles, despite a slight fluctuation observed in the voltage-time profiles. The small voltage hysteresis between deposition and dissolution is a good indicator of the facile electrode kinetics. The current densities employed here correspond to C/2~5C rate for a cell of a nominal areal capacity of 2 mAh cm^{-2}, which are sufficient for most practical applications.[46] As shown by ex-situ SEM images, cycled Zn electrode is fairly dense and dendrite-free, while energy dispersive X-ray spectroscopy (EDX) and XRD patterns reveal that the deposited element is exclusively metallic Zn (Figue S7). It is evident that the molten hydrate electrolyte offers the opportunities for Zn anode to achieve satisfactory coulombic efficiency, rate capability, and long cycle life over a wide current range. To the best of our knowledge, this is the first demonstration of a Zn anode with such a long-term cyclability. Of interest is the fact that these results are achieved under a lean electrolyte condition (i.e., minimum amount of electrolyte),[17] which is desirable for heightening the cell-level energy density of Zn-based rechargeable battery. Besides, it can be seen that the cyclability of Zn anode in $ZnCl_2 \cdot 2.33H_2O$ exceeds those using $ZnCl_2 \cdot 3H_2O$ and $ZnCl_2 \cdot 4H_2O$ (Figure S8). These data illustrate that the bulk ionic conductivity of electrolyte is not a key requirement for stable Zn deposition/stripping performance, but more likely the solution structure as discussed above. Under the same condition, the Zn/Zn cell using the alkaline electrolyte exhibited much worse cyclability (Figure S9a). It shows obvious voltage oscillation over time, which eventually leads to cell failure at 150 h at a current density of 1 mA cm^{-2} and only 80 h at a current density of 5 mA cm^{-2}. Terminal failure observed here could be ascribed to the depletion of reducible Zn species and electrode surface passivation owing to the accumulation of needle-like, insulating zinc oxide as

evidenced by ex-situ XRD and SEM analysis (Figure S9b and c). The formation of zinc oxide is consistent with previous reports.[4,20]

It was well-documented that Zn experiences high dissolution and corrosion in alkaline aqueous electrolytes.[13,14] The former leads to the growth of dendrites and electrode shape change, whereas the latter is associated to the hydrogen evolution reaction on the Zn surface.[13] All these phenomena deteriorate the effective utilization and reversibility of the Zn anode; however, they have not been seriously considered since the amount of Zn anode is usually excessive as compared to the cathode of interest, both in Zn-ion or Zn–air batteries.[21] To shed light on the stability of Zn anode in the molten hydrate and the influence of ambient exposure to the electrolyte, immersion test was conducted using Zn/Zn coin cells with air access holes. Electrochemical impedance spectroscopy (EIS) was undertaken for the cells before and after immersion in order to monitor the change in electrode surface state. For the cell adopting $ZnCl_2 \cdot 2.33H_2O$, the interfacial resistance was kept almost constant for 30 days (Figure S10a and b), which is reflected to the absence of crystalline corrosion product on Zn electrode (Figure S10c). Most importantly, the cell exhibits nearly the identical deposition/dissolution behavior after the immersion test, which ascertaining the integrity of both Zn electrodes and the electrolyte (Figure S10d). In sharp contrast, surface state of Zn in the alkaline electrolyte continuously varied during immersion as shown by the noisy voltage-time profile and amplified interfacial resistance (Figure S11a and b), which was confirmed by the precipitated ZnO (Figure S11c). As show in Figure S12, SEM images of Zn electrodes recovered from two electrolytes clearly reveal that self-corrosion is suppressed in $ZnCl_2 \cdot 2.33H_2O$, which is attributed to the strong hydration effect in the molten hydrate that significantly decreased the water activity.[28]

It is important to underline that most of the previous studies on alkaline Zn–air batteries using flooded cells with an enormous electrolyte volume (see Ref. 47 for clarity). However, it is increasingly recognized now that electrochemical properties obtained in this manner cannot represent the true performance in practical batteries in which a reasonable electrolyte content is

required for better volumetric and gravimetric energy densities.[17,48] Bearing this in mind, a Zn–air cell using $ZnCl_2 \cdot 2.33H_2O$ electrolyte was constructed with Zn as the anode and Pt/C catalyst as the cathode. The set-up is schematically illustrated in **Figure 4**a. The cell exhibits an open-circuit potential of ca. 1.4 V, which is close to the values reported in the alkaline solution.[8–11] A flat discharge curve at ca. 1.2 V and a high specific capacity exceeding 10000 mAh g^{-1} are achieved at 100 mA g^{-1}, on the basis of the weight of Pt in the cathode (Figure S13a). The end of discharge observed here is believed to be related to either kinetic restriction of the catalyst[12] and/or limited oxygen diffusion into the air electrode owing to the increase in electrolyte viscosity as a result of continuous Zn dissolution. As shown in Figure S13b, the potential gap between discharge and charge increases with increasing current density. Especially, the charge polarization degree is more sensitive to applied current, highlighting the importance of catalysts for OER. Nevertheless, the cell could persistently deliver a stable capacity for 100 cycles under a constant-capacity mode of 1000 mAh g^{-1} at 500 mA g^{-1} (Figure 4b). The cycle performance measured at 200 and 1000 mA g^{-1} is shown in Figure S13c and d. Since the Zn anode remains intact after the cycling in Zn–air batteries (Figure S14), the increasing potential gap upon cycling is caused by the degradation of the cathode. Catalyst aggregation and loss of porosity were observed for the cycled air electrode (Figure S15). Because ORR mainly occurs at three-phase sites among oxygen (gas), electrolyte (liquid), and catalyst (solid), porous structure of cathode acting as oxygen channels is very crucial. [12] On the other hand, OER occurs at the interface between electrolyte and catalyst; namely, a porous structure is not essential. This is why the discharge overpotential increased upon cycling while the charging curves remain almost unchanged. Despite the limited amount of electrolyte applied, the cyclability and sustained operation time (> 400 h) of the present cell is better than other Zn–air batteries in the literature. It is postulated that the favorable anodic reaction and chemical stability of Zn within Zn molten hydrate synergistically contribute to the good durability. To clarify the cathodic reaction, ex-situ analysis was conducted. SEM, EDX and XRD results

clearly depict that ZnO was formed after the first discharge process (Figure 4c and S16a). These discharge products are pillar shaped with a hexagonal cross-section and their size are ranging from few tens to several hundred of nanometers (Figure S16b). ZnO could be effectively decomposed and virtually disappeared after the charge, assuring the rechargeable Zn–air cell utilizing a molten hydrate electrolyte involves the reversible formation of ZnO (Figure 4d and S16a). It is worth noting that this reaction mechanism is distinct to the one using alkaline electrolytes, in which the formation of zincate ions ($Zn(OH)_4^{2-}$) predominants.[12] Besides, gas analysis after discharge-charge test was carried out to trace possible formation of chlorine gas from $ZnCl_2 \cdot 2.33H_2O$. The result revealed that the electricity qauntity consumed for chlorine gas evolution was less than 0.8% (see Supporting Information for details of the calculation). It is well-known that the chlorine gas evolution potential will shift to more positive as forming chlorozincate complexes ($[ZnCl_4]^{2-}$ or large cluster).[49] Nevertheless, further improvement in terms of cycling stability and energy efficiency is expectable with the utilization of advanced bifunctional catalyst[50,51], especially those possessing selective oxygen evolution catalytic activity.[52] Additional positive feature of the $ZnCl_2 \cdot 2.33H_2O$ electrolyte is verified from the discharge-charge experiment conducted in a dry air environment, using the same cell setup. The results demonstrate an enhanced cyclability compared with that using a conventional alkaline electrolyte (6 M KOH-0.2 M $ZnCl_2$), which shows severe capacity loss after only 4 cycles (Figure S17). The enhancement presumably originates from two aspects, the better carbon dioxide tolerance than alkaline solution, as well as the greater water-retention capability endowed by the strong hydration effect between Zn^{2+} and water.

In conclusion, we investigated the $ZnCl_2$–H_2O system as the electrolytes for Zn–air battery and unveiled the crucial role of the water content. The concentrated state, $ZnCl_2 \cdot 2.33H_2O$, referring to a Zn molten hydrate, offers a suite of unique properties that were unachievable with its diluted counterparts. The resultant Zn–air cell is demonstrated to show a potential high energy density and a good cyclability, which are enabled by the highly reversible Zn

deposition/dissolution, as well as the chemically stable Zn interface, both of which are consequence of the peculiar solution structure and strong hydration effect exclusive for Zn molten hydrate. Revisiting other low-melting inorganic molten hydrates and leveraging our new insights will facilitate the development of new electrolyte materials of unique properties and cost effectiveness.

Supporting Information
Supporting Information is available from the Wiley Online Library or from the author.

Acknowledgements
We express our gratitude to the reviewers for valuable suggestions and the National Institute of Advanced Industrial Science and Technology (AIST) for financial support.

Received: ((will be filled in by the editorial staff))
Revised: ((will be filled in by the editorial staff))
Published online: ((will be filled in by the editorial staff))

References

[1] R. Schmuch, R. Wagner, G. Horpel, T. Placke, M. Winter, *Nat. Energy* **2018**, *3*, 267.

[2] J. H. Wang, Y. Yamada, K. Sodeyama, E. Watanabe, K. Takada, Y. Tateyama, A. Yamada, *Nat. Energy* **2018**, *3*, 22.

[3] D. Kundu, B. D. Adams, V. D. Ort, S. H. Vajargah, L. F. Nazar, *Nat. Energy* **2016**, *1*, 16119.

[4] H. L. Pan, Y. Y. Shao, P. F. Yan, Y. W. Cheng, K. S. Han, Z. M. Nie, C. M. Wang, J. H. Yang, X. L. Li, P. Bhattacharya, K. T. Mueller, J. Liu, *Nat. Energy* **2016**, *1*, 16039.

[5] N. Zhang, F. Y. Cheng, J. X. Liu, L. B. Wang, X. H. Long, X. S. Liu, F. J. Li, J. Chen, *Nat. Commun*. **2017**, *8*, 405.

[6] F. Wang, E. Y. Hu, W. Sun, T. Gao, X. Ji, X. L. Fan, F. D. Han, X. Q. Yang, K. Xu, C. S. Wang, *Energy Environ. Sci*. **2018**, *11*, 3168.

[7] J. W. Ding, Z. G. Du, L. Q. Gu, B. Li, L. Z. Wang, S. W. Wang, Y. J. Gong, S. B. Yang, *Adv. Mater*. **2018**, *30*, 1800762.

[8] J. Yin, Y. X. Li, F. Lv, Q. H. Fan, Y. Q. Zhao, Q. L. Zhang, W. Wang, F. Y. Cheng, P. X. Xi, S. J. Guo, *ACS Nano* **2017**, *11*, 2275.

[9] Y. J. Li, L. Cui, P. F. Da, K. W. Qiu, W. J. Qin, W. B. Hu, X. W. Du, K. Davey, T. Ling, S. Z. Qiao, *Adv. Mater*. **2018**, *30*, 1804653.

[10] C. Tang, B. Wang, H. F. Wang, Q. Zhang, *Adv. Mater*. **2017**, *29*, 1703185.

[11] L. L. Zhou, C. C. Hou, Z. Liu, H. Pang, Q. Xu, *J. Am. Chem. Soc*. **2018**, *140*, 15393.

[12] J. Fu, Z. P. Cano, M. G. Park, A. P. Yu, M. Fowler, Z. W. Chen, *Adv. Mater*. **2017**, *29*, 1604685.

[13] A. R. Mainar, E. Iruin, L. C. Colmenares, A. Kvasha, I. D. Meatza, M. Bengoechea, O. Leonet, I. Boyano, Z. Zhang, J. A. Blazquez, *J. Energy Storage*, **2018**, *15*, 304.

[14] A. L. Zhu, D. P. Wilkinson, X. E. Zhang, Y. L. Xing, A. G. Rozhin, S. A. Kulinich, *J. Energy Storage* **2016**, *8*, 35.

[15] N. Zhang, F. Y. Cheng, Y. C. Liu, Q. Zhao, K. X. Lei, C. C. Chen, X. S. Liu, J. Chen, *J. Am. Chem. Soc*. **2016**, *138*, 12894.

[16] C. Zhang, J. Holoubek, X. Y. Wu, A. Daniyar, L. D. Zhu, C. Chen, D. P. Leonard, I. A. Rodriguez-Perez, J. X. Jiang, C. Fang, X. Ji, *Chem. Commun*. **2018**, *54*, 14097.

[17] Y. T. Wu, Y. M. Zhang, Y. Ma, J. D. Howe, H. C. Yang, P. Chen, S. Aluri, N. Liu, *Adv. Energy Mater.* **2018**, *8*, 1802470.

[18] W. Li, K. L. Wang, M. Zhou, H. C. Zhan, S. J. Cheng, K. Jiang, *ACS Appl. Mater. Interfaces* **2018**, *10*, 22059.

[19] K. N. Zhao, C. X. Wang, Y. H. Yu, M. Y. Yan, Q. L. Wei, P. He, Y. F. Dong, Z. Y. Zhang, X. D. Wang, L. Q. Mai, *Adv. Mater. Interfaces* **2018**, *5*, 1800848.

[20] F. Wang, O. Borodin, T. Gao, X. L. Fan, W. Sun, F. D. Han, A. Faraone, J. A. Dura, K. Xu, C. S. Wang, *Nat. Mater*. **2018**, *17*, 543.

[21] M. Song, H. Tan, D. L. Chao, H. J. Fan, *Adv. Funct. Mater*. **2018**, *28*, 1802564.

[22] F. Mylius, R. Dietz, *Z. Anorg. Chem*. **1905**, *44*, 209.

[23] J. Braunstein, *Inorg. Chim. Acta Rev*. **1968**, *2*, 19.

[24] C. A. Angell, Y. Ansari, Z. F. Zhao, *Faraday Discuss*. **2012**, *154*, 9.

[25] R. J. Wilcox, B. P. Losey, J. C. W. Folmer, J. D. Martin, M. Zeller, R. Sommer, *Inorg. Chem*. **2015**, *54*, 1109.

[26] L. M. Suo, O. Borodin, T. Gao, M. Olguin, J. Ho, X. L. Fan, C. Luo, C. S. Wang, K. Xu, *Science* **2015**, *350*, 938.

[27] V. A. Azov, K. S. Egorova, M. M. Seitkalieva, A. S. Kashina, V. P. Ananikov, *Chem. Soc. Rev*. **2018**, *47*, 1250.

[28] Y. Yamada, K. Usui, K. Sodeyama, S. Ko, Y. Tateyama, A. Yamada, *Nat. Energy* **2016**, *1*, 16129.

[29] Y. Marcus, *Ionic liquid properties. From molten salts to RTILs*, Springer, Switzerland, **2016**, pp.109–122.

[30] S. D. Han, N. N. Rajput, X. H. Qu, B. F. Pan, M. N. He, M. S. Ferrandon, C. Liao, K. A. Persson, A. K. Burrell, *ACS Appl. Mater. Interfaces* **2016**, *8*, 3021.

[31] Z. Liu, G. Pulletikurthi, A. Lahiri, T. Cui, F. Endres, *Dalton Trans*. **2016**, *45*, 8089.

[32] M. Chamoun, B. J. Hertzberg, T. Gupta, D. Davies, S. Bhadra, B. Van Tassell, C. Erdonmez, D. A. Steingart, *NPG Asia Mater*. **2015**, *7*, e178.

[33] M. Mizuhata, Y. Sumihiro, S. Deki, *Phys. Chem. Chem. Phys*. **2004**, *6*, 1944.

[34] M. Watanabe, M. L. Thomas, S. G. Zhang, K. Ueno, T. Yasuda, K. Dokko, *Chem. Rev*. **2017**, *117*, 7190.

[35] K. Xu, *Chem. Rev*. **2018**, *114*, 11503.

[36] D. E. Irish, T. F. Young, B. McCarroll, *J. Chem. Phys*. **1963**, *39*, 3436.

[37] T. Yamaguchi, S. Hayashi, H. Ohtaki, *J. Phys. Chem*. **1989**, *93*, 2620.

[38] H. Kanno, J. Hiraishi, *J. Raman Spectrosc*. **1980**, *9*, 85.

[39] M. Ahmed, V. Namboodiri, A. K. Singh, J. A. Mondal, *J. Chem. Phys*. **2014**, *141*, 164708.

[40] G. Maisano, P. Migliardo, M. P. Fontana, M. C. Bellissent-Funel, A. J. Dianoux, *J. Phys. C: Solid State Phys*. **1985**, *18*, 1115.

[41] L. M. Uriarte, J. Dubessy, P. Boulet, V. G. Baonza, I. Bihannic, P. Robert, *J. Raman Spectrosc*. **2015**, *46*, 822.

[42] D. E. Irish, T. F. Young, *J. Chem. Phys*. **1965**, *43*, 1765.

[43] A. C. Harris, H. N. Parton, *Trans. Faraday Soc*. **1940**, *36*, 1139.

[44] J. Jorne, W. T. Ho, *J. Electrochem. Soc*. **1982**, *129*, 907.

[45] G. Y. Zheng, S. W. Lee, Z. Liang, H. W. Lee, K. Yan, H. B. Yao, H. T. Wang, W. Y. Li, S. Chu, Y. Cui, *Nat. Nanotechnol*. **2014**, *9*, 618.

[46] S. R. Chen, J. M. Zheng, D. H. Mei, K. S. Han, M. H. Engelhard, W. G. Zhao, W. Xu, J. Liu, J. G. Zhang, *Adv. Mater.* **2018**, *30*, 1706102.

[47] D. Stock, S. Dongmo, K. Miyazaki, T. Abe, J. Janek, D. Schroder, *J. Power Sources* **2018**, *395*, 195.

[48] P. Chen, Y. T. Wu, Y. M. Zhang, T. H. Wu, Y. Ma, C. Pelkowski, H. C. Yang, Y. Zhang, X. W. Wu, N. Liu, *J. Mater. Chem. A* **2018**, *6*, 21933.

[49] S. I. Hsiu, J. F. Huang, I. W. Sun, C. H. Yuan, J. Shiea, *Electrochim. Acta* **2002**, *47*, 4367.

[50] J. Pan, Y. Y. Xu, H. Yang, Z. H. Dong, H. F. Liu, B. Y. Xia, *Adv. Sci*. **2018**, *5*, 1700691.

[51] H. F. Wang, C. Tang, Q. Zhang, *Adv. Funct. Mater*. **2018**, *28*, 1803329.

[52] J. G. Vos, T. A. Wezendonk, A. W. Jeremiasse, M. T. M. Koper, *J. Am. Chem. Soc*. **2018**, *140*, 10270.

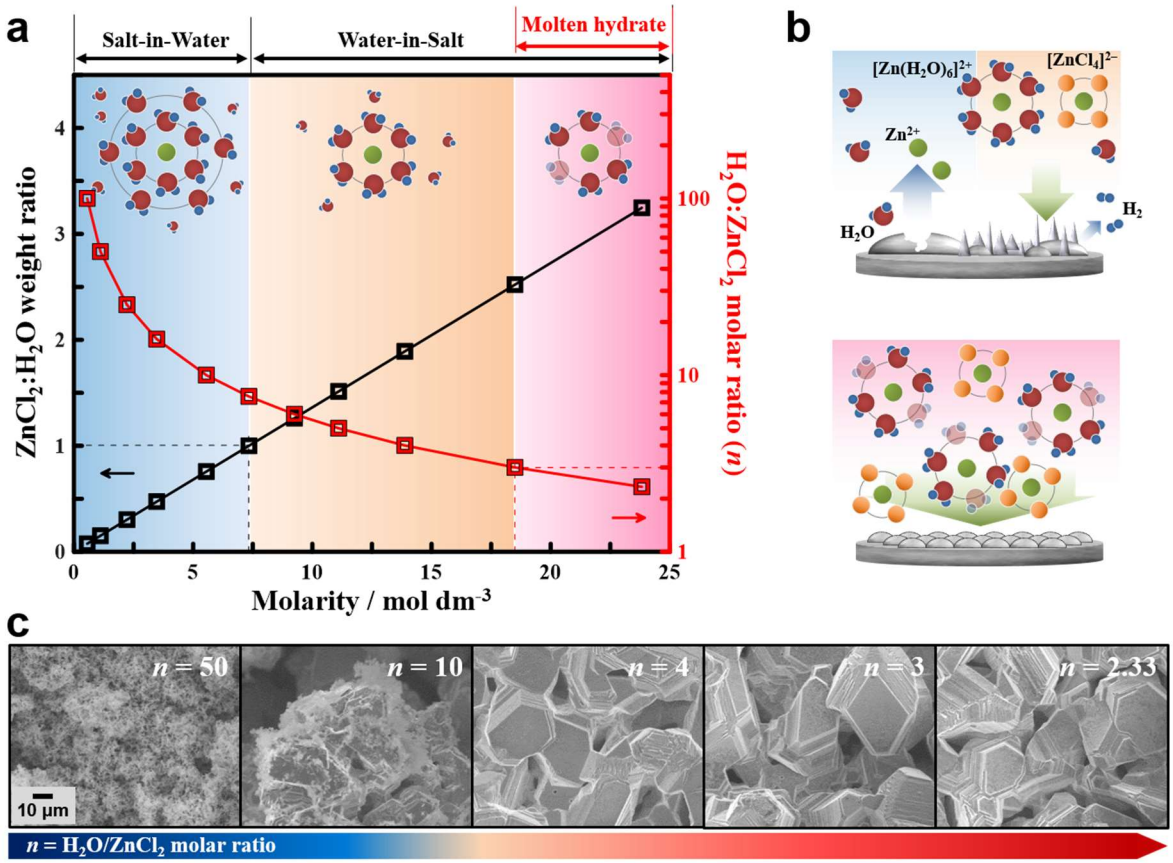

Figure 1. (a) Molarity of the $ZnCl_2$–H_2O binary system as functions of the weight ratio of $ZnCl_2$ to H_2O and the molar ratio of H_2O to $ZnCl_2$ (n). The prospective hydration shells around Zn are shown as inset. The term "water-in-salt" denotes electrolyte with salt to water weight ratio > 1. (b) Schematic illustration of (top) Zn dendrite growth, shape change, and hydrogen evolution in conventional electrolytes and (bottom) Zn deposition in a molten hydrate electrolyte, in which uniform ion distribution promotes smooth deposition and less uncoordinated water alleviates hydrogen evolution. (c) SEM images of Zn deposits obtained by constant voltage deposition on Ni substrates at –0.2 V (vs Zn/Zn^{2+}) for 1 h at 30 °C.

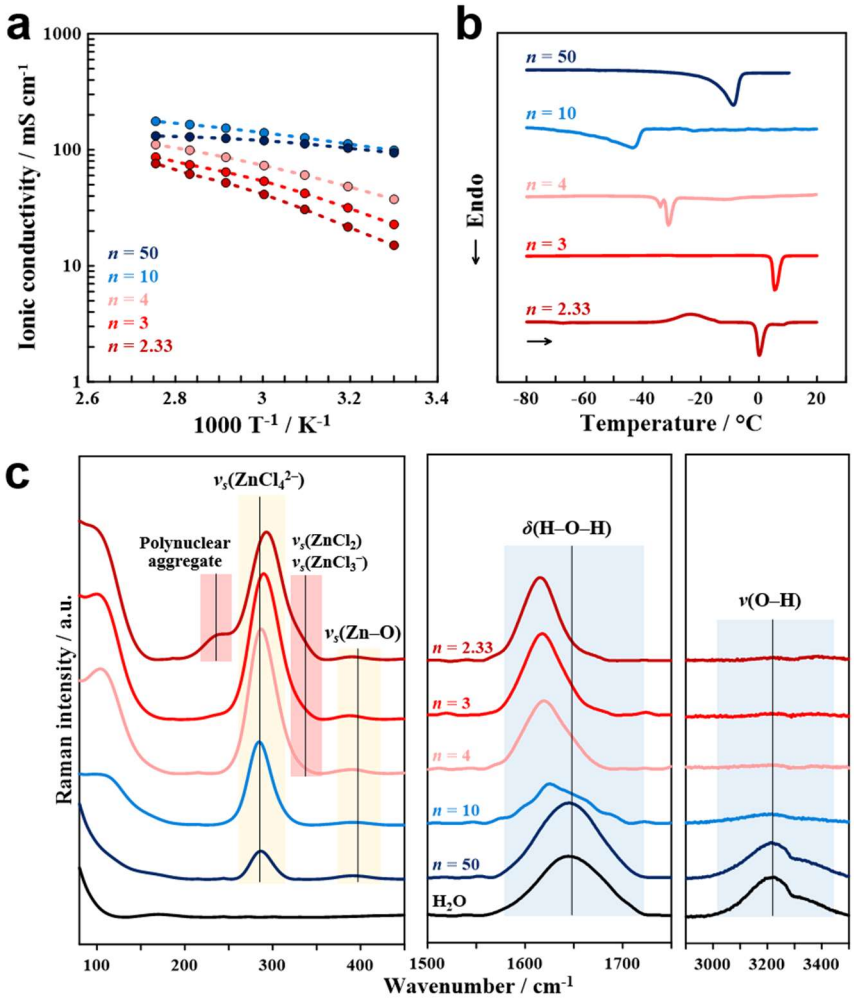

Figure 2. (a) Temperature (T) dependence of ionic conductivity of $ZnCl_2 \cdot nH_2O$. (b) DSC thermograms of $ZnCl_2 \cdot nH_2O$ recorded at 2 °C min^{-1}. (c) Raman spectra of $ZnCl_2 \cdot nH_2O$ in which ν and δ represent stretching and bending modes, respectively.

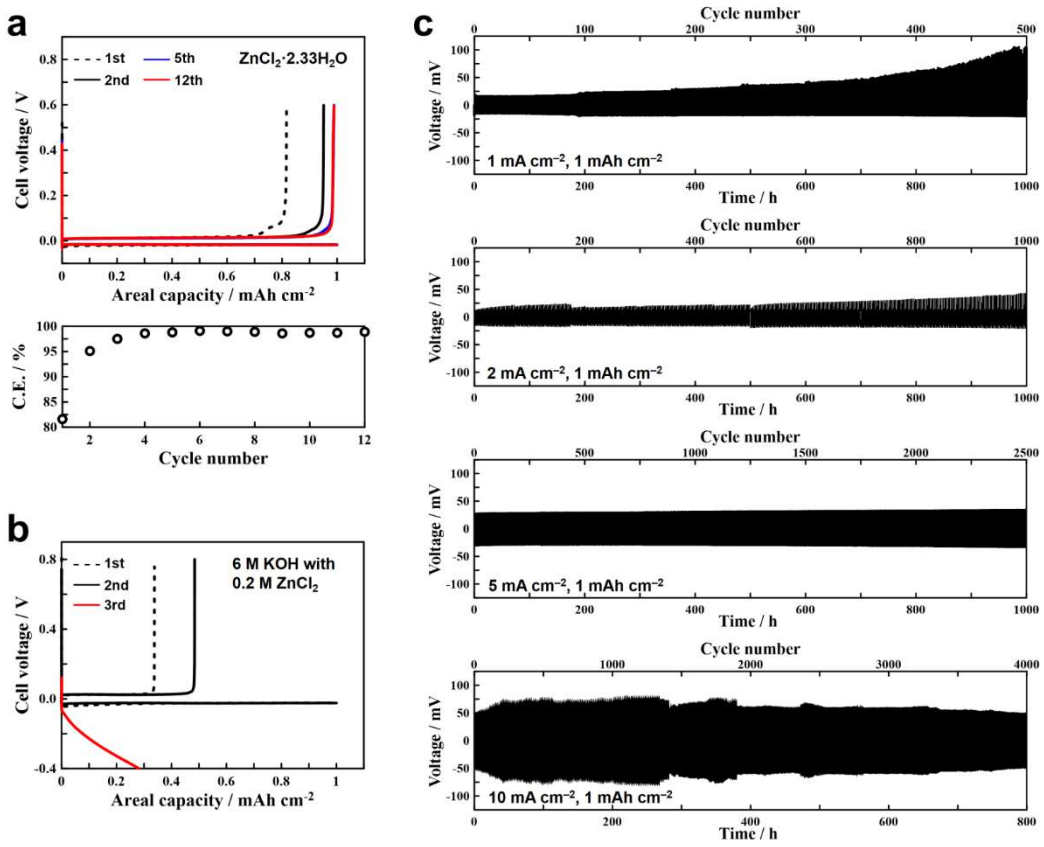

Figure 3. Galvanostatic Zn deposition-stripping in a Zn/Mo cell in (a) $ZnCl_2·2.33H_2O$ and (b) 6 M KOH-0.2 M $ZnCl_2$. (c) Cycling performance of Zn/Zn symmetric cells in $ZnCl_2·2.33H_2O$ at various current densities with a fixed areal capacity of 1 mAh cm^{-2}. Operating temperature: 30 °C.

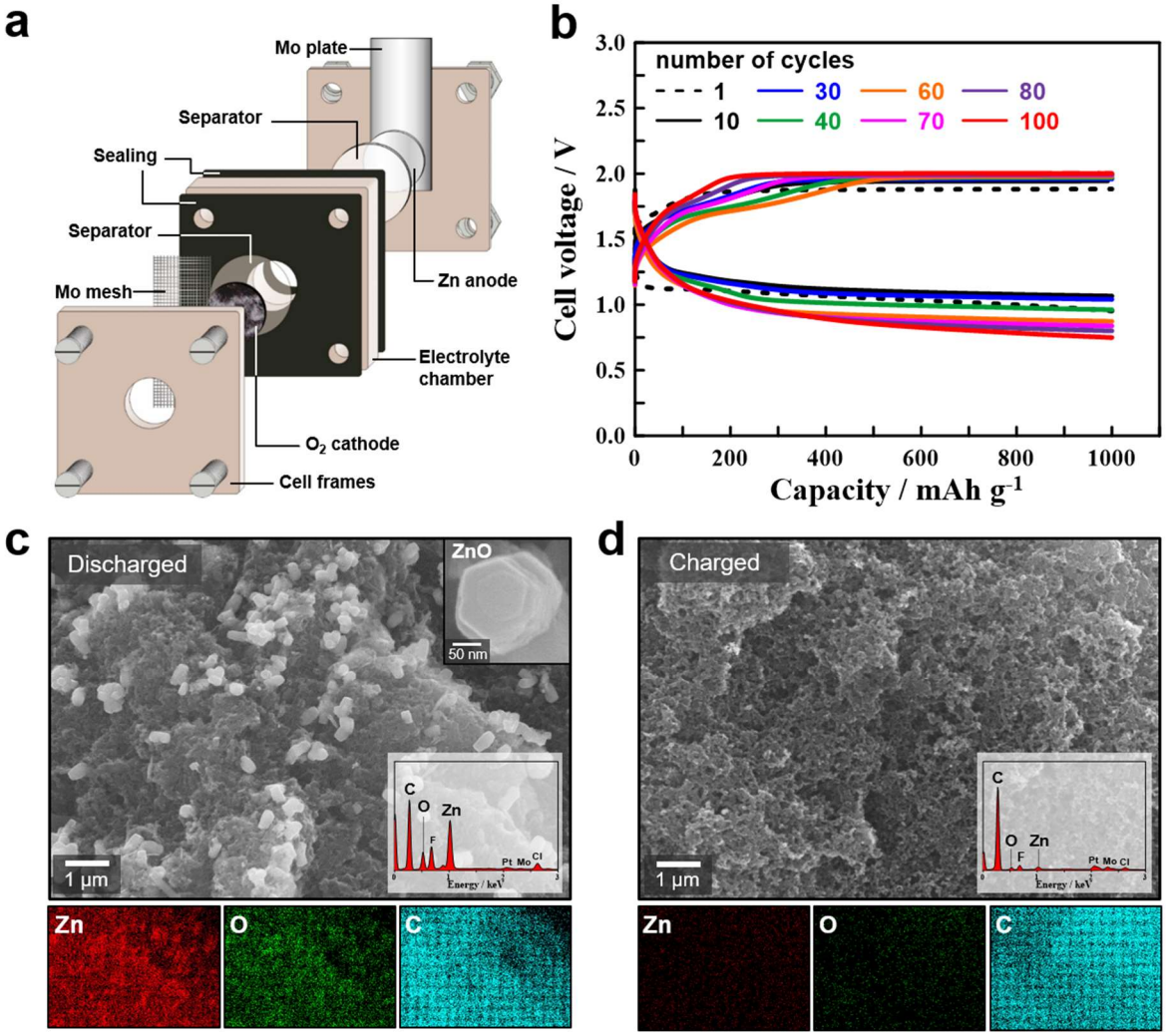

Figure 4. (a) The schematic drawing of Zn–air cell set up in which the cathode is 50% Pt/C loaded on a gas diffusion layer and the anode is Zn plate. (b) Cycling performance of the Zn–air cell at a current density of 500 mA g^{-1} under a constant-capacity mode (mass based on Pt, 1000 mAh g^{-1} corresponds to a cathodic areal capacity of 0.5 mAh cm^{-2}). Operating condition: oxygen-filled, 30 °C. SEM images, EDX analysis and elemental mapping of the Pt/C cathodes at (c) the discharge state and (d) the charge state. The inset inf (c) shows the hexagonal microstructure of discharge product ZnO formed in the Zn–air cell.

Zinc molten hydrate electrolyte is demonstrated to be an advantageous electrolyte for Zn-based battery applications. The high Zn concentration and reduced water activity not only promote dendrite-free Zn plating/stripping at a high coulombic efficiency but also effectively suppress self-corrosion of Zn, enabling Zn–air batteries a long-term cyclability.

Keyword
molten hydrates, ionic liquids, zinc anodes, aqueous batteries, zinc–air batteries
C. Y. Chen, K. Matsumoto, K. Kubota,* R. Hagiwara, Q. Xu*

A Room-Temperature Molten Hydrate Electrolyte for Rechargeable Zinc–Air Batteries